nature climate change

LETTERS

PUBLISHED ONLINE: 8 AUGUST 2016 | DOI: 10.1038/NCLIMATE3092

Revegetation in China's Loess Plateau is approaching sustainable water resource limits

Xiaoming Feng[1,2], Bojie Fu[1,2]*, Shilong Piao[3,4], Shuai Wang[1,2], Philippe Ciais[5], Zhenzhong Zeng[3], Yihe Lü[1,2], Yuan Zeng[6], Yue Li[3], Xiaohui Jiang[7] and Bingfang Wu[6]

Revegetation of degraded ecosystems provides opportunities for carbon sequestration and bioenergy production[1,2]. However, vegetation expansion in water-limited areas creates potentially conflicting demands for water between the ecosystem and humans[3]. Current understanding of these competing demands is still limited[4]. Here, we study the semi-arid Loess Plateau in China, where the 'Grain to Green' large-scale revegetation programme has been in operation since 1999. As expected, we found that the new planting has caused both net primary productivity (NPP) and evapotranspiration (ET) to increase. Also the increase of ET has induced a significant ($p < 0.001$) decrease in the ratio of river runoff to annual precipitation across hydrological catchments. From currently revegetated areas and human water demand, we estimate a threshold of NPP of 400 ± 5 g C m^{-2} yr^{-1} above which the population will suffer water shortages. NPP in this region is found to be already close to this limit. The threshold of NPP could change by −36% in the worst case of climate drying and high human withdrawals, to +43% in the best case. Our results develop a new conceptual framework to determine the critical carbon sequestration that is sustainable in terms of both ecological and socio-economic resource demands in a coupled anthropogenic–biological system.

Revegetation programmes aim to restore degraded ecosystem services, by improving carbon sequestration, soil conservation and reducing floods[5]. Newly planted vegetation can also contribute to climate change mitigation both by storing carbon, and by providing biofuel for bioenergy production[3]. Globally, future carbon sequestration from new forests was estimated by the Intergovernmental Panel on Climate Change 5th Assessment Report (IPCC AR5) to range from 40 to 70 Pg C by 2100[6]. However, newly planted vegetation needs water, nutrients, light and CO_2 to grow[4]. The water demand of the newly planted ecosystem is of particular concern in the seasonally dry areas that cover 47% of the global land area[2]. In these areas, ecosystems and human activities both depend on the same source of water, namely precipitation[7]. Revegetation programmes in these regions create potentially conflicting demands for water between ecosystems and humans. Hence, balancing vegetation productivity and water use by humans is critical to promoting sustainable management of the revegetation programmes and safeguarding the water demand of the socio-economic system.

The Grain to Green Programme (GTGP) of the Loess Plateau of China (see Methods) is the largest ecological restoration programme ever implemented in a developing country[8]. The result is a uniquely massive experiment of vegetation plantation. Since 1999, approximately US$8.7 billion has been invested to convert previously cultivated land to perennial non-native vegetation (see Supplementary Notes)[5]. Creating a return on this investment, while ensuring that the revegetation is ecologically sustainable, is a substantial challenge[9]. Historically, intensive agricultural practices that peaked in the 1970s have led to the Loess Plateau region having very eroded soils[8]. The GTGP has converted 16,000 km^2 of rain-fed cropland to planted vegetation, causing a 25% increase in vegetation cover during the last decade (Fig. 1). Precipitation is needed to sustain the newly planted ecosystem, but water is also required by the 108 million people living in the region. The water demand from the residential, agricultural and industrial sectors has increased by 4% per year over the same time as the area of new planting has expanded, and only 30% of this water demand is met from sources outside the region (see Supplementary Notes and Supplementary Figs 1 and 2). Thus, determining the regional tolerance of vegetation productivity is a prerequisite to finding a balanced solution of ecosystem restoration and water reduction for this area, and ensuring that the revegetation is socially and ecologically sustainable.

We analysed vegetation productivity changes and regional ET in the Loess Plateau over the lifetime of the GTGP, using observations of the Moderate Resolution Imaging Spectro-radiometer (MODIS) and simulations from the models derived by satellite data (see Methods). Total regional NPP is estimated to have increased by 9.3 ± 1.3 g C m^{-2} yr^{-1} (+35%; $p < 0.001$) during 2000–2010 (Fig. 1c). Accordingly, satellite-derived ET estimates increased by 4.3 ± 1.7 mm yr^{-2} ($p = 0.04$) over the last decade (Fig. 2a), a figure that is consistent with, although lower than, the independent trend of ET inferred from the water balance of the Loess Plateau area (6.8 ± 3.8 mm yr^{-2}; yellow bar in Fig. 2a; see Methods for ET derived from water balance data).

The spatial extent of the greening trend observed from MODIS coincides with the GTGP plantations (Fig. 1b,c); changes in NPP from the Carnegie–Ames–Stanford approach ecosystem model (see Methods) in other ecosystems are generally less significant (Fig. 1c). Similarly, the sub-regional areas of ET increase coincide with the new plantations (Figs 1b and 2a). Annual ET estimated from the areas without revegetation does not show any significant trend (Fig. 2a). These results show that land-use change rather than climatic and/or environmental change is the primary cause for the estimated increase of annual NPP or ET for the Loess Plateau. The

[1]State Key Laboratory of Urban and Regional Ecology, Research Center for Eco-Environmental Sciences, Chinese Academy of Sciences, Beijing 100085, China. [2]Joint Center for Global Change Studies, Beijing 100875, China. [3]College of Urban and Environmental Sciences, Peking University, Beijing 100871, China. [4]Institute of Tibetan Plateau Research, Chinese Academy of Sciences, Beijing 100101, China. [5]Laboratoire des Sciences du Climat et de l'Environnement (LSCE), CEA CNRS UVSQ, 91191 Gif-sur-Yvette, France. [6]Institute of Remote Sensing and Digital Earth, Chinese Academy of Sciences, Beijing 100094, China. [7]Yellow River Institute of Hydraulic Research, YRCC, Zhengzhou 450003, China. *e-mail: bfu@rcees.ac.cn

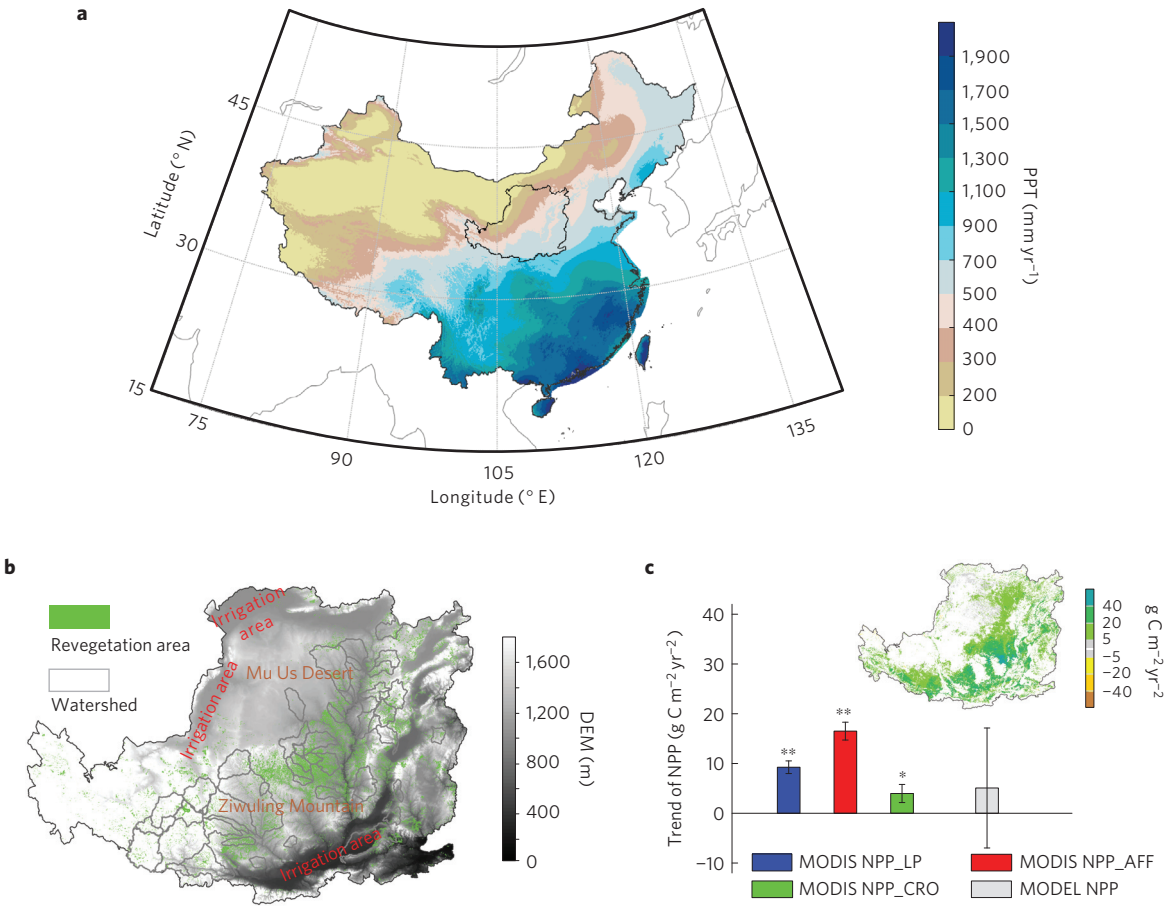

Figure 1 | Location of the Loess Plateau and change in vegetation. a, Mean annual precipitation (PPT) over 2000–2010. **b**,Distribution of revegetated areas and the hydrological catchments. **c**, Annual NPP trend of the whole plateau (MODIS NPP_LP), the revegetated areas (MODIS NPP_AFF), the adjacent unconverted cropland (MODIS NPP_CRO, Supplementary Fig. 8) and the general ecosystem model simulation (MODEL NPP). Asterisks above the bars indicate that the trend is statistically significant at the $p < 0.01$ (**) and $p < 0.05$ (*) level, respectively. The inset shows the spatial pattern of annual NPP change, with white indicating those areas with no significant change ($p > 0.05$). Error bars are the standard deviation across years.

credibility of this analysis is also supported by a test with four different terrestrial ecosystem models (see Methods). When only the effects of climate, CO_2 and nitrogen deposition were included (that is, land-use change not included), the models reproduced averaged NPP ($5.1 \pm 12.1\,g\,C\,m^{-2}\,yr^{-1}$, $p = 0.68$) and ET trends ($1.1 \pm 2.8\,mm\,yr^{-1}$, $p = 0.71$), encapsulating the climatic and/or environmental effects. These model results support the contention that revegetation is the main cause of the satellite-observed NPP and ET increase.

River discharge data from 32 hydrological catchments in the region, where 1–26% of the area had been revegetated since 1999, allow us to draw a picture of the regional runoff change. Water yield (that is, the ratio of annual river runoff to precipitation) averaged across the observed catchments dropped from 8% during the period of 1980 to 1999 (that is, before the plantations), to 5% during 2000–2010. Before planting (1980–1999), annual runoff was spatially and significantly positively correlated with annual precipitation ($R^2 = 0.29$, $p < 0.001$); but for 2000–2010, if there was planting, low runoff (that is, less than $20\,mm\,yr^{-1}$) also occurred with relatively high precipitation of 400–550 $mm\,yr^{-1}$ (Fig. 2b).

Revegetation increasing ET implies a decrease in runoff and soil water availability, because precipitation input has not significantly increased during the last decade[4,10] (see Supplementary Fig. 3). The reduction in runoff caused by vegetation planting is illustrated by the positive spatial correlation between the change of annual runoff and both leaf area index (LAI) change and revegetated area over the different catchments (Fig. 2b). The significant, but still relatively small contribution, of LAI change to the observed spatial distribution of runoff decrease suggests the importance of other factors (for example, seasonal variations, soil water holding capacities and fertility, species-specific water-use efficiency, tree rooting depth). For example, it has been suggested that revegetation starts to decrease streamflow within a few years of planting and the decreasing trend continues for approximate 30 years[4], as trees grow older and evaporate more. Due to the lack of detailed information about the spatial distribution of plantation age, Fig. 2b indirectly includes impacts of plantation age on runoff change through changes in LAI (see the LAI increment after revegetation in Supplementary Fig. 4). It should be noted, however, that LAI for a young plantation in the study area is generally significantly and positively related to plant age[10–12]. But the spatial pattern of runoff change was not significantly correlated with precipitation change ($R^2 = 0.02$, $p > 0.2$). We also found that the effect of dams and terrace construction[13–15] on runoff reduction between the 1980s and 2000s is not significant ($p > 0.1$; Supplementary Table 1)[16]. Figure 2b indicates that soil moisture also decreased in all revegetated catchments. The relationships between change in runoff and change in soil water with revegetated area and change in LAI are shown in Fig. 2b. We extrapolated these relationships to the 16,000 km^2 (2.5% by area) of new planting on the Loess Plateau that coincided with an increase of LAI of 0.07 since 1999. Over 2000–2010, the revegetation translates into a loss of $2.4 \pm 0.9\,mm\,yr^{-1}$ ($p = 0.08$) of soil moisture and $0.5 \pm 0.3\,mm\,yr^{-1}$ ($p = 0.006$) of runoff. Assuming that the reduction of both soil moisture and runoff was entirely used to sustain an increase of ET,

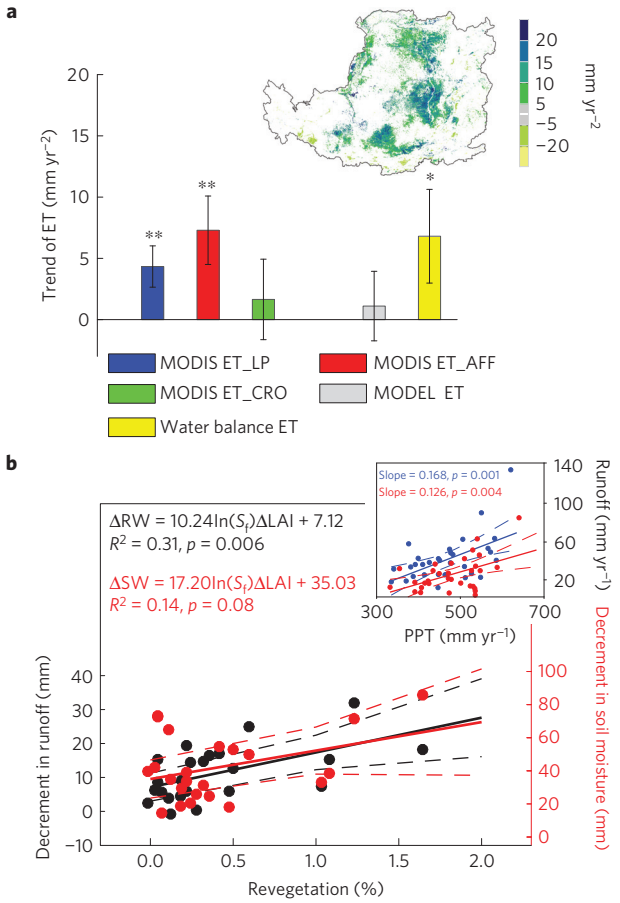

Figure 2 | Changes in NPP and water resources. a, Same as Fig. 1c, but for annual ET trend; water balance ET derived as a residual in the water balance is included. **b**, The relationship between runoff decrease (ΔRW, mm) and the revegetation indicated by revegetated area (S_f) and LAI change (ΔLAI); and for soil water decrease (ΔSW). The inset shows the change in the relationship between runoff and precipitation before and after revegetation (see Supplementary Fig. 11 for the catchments included), with data shown for before plantations (1980–1999, blue), and after plantations (2000–2010, red). The dashed lines in **b** and its inset denote the 95% confidence intervals of the regressions.

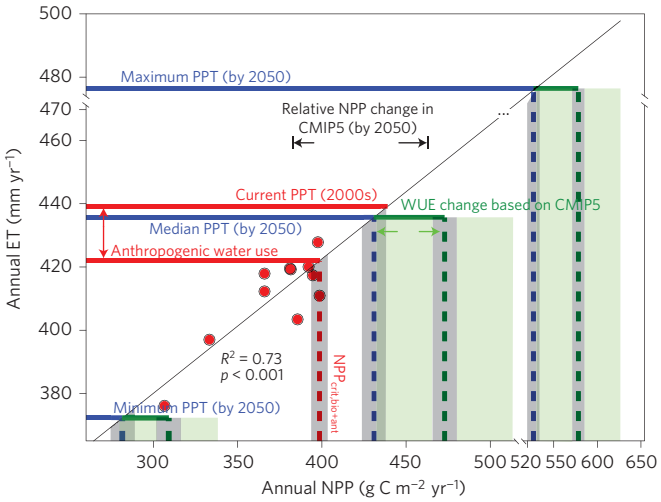

Figure 3 | NPP thresholds derived from the satellite-observed NPP–ET relationship and the predictions of $NPP_{crit,bio+ant}$ for the climate of the 2050s. The output of 30 GCMs from IPCC AR5 under the RCP4.5 scenario was used. Areas shaded in grey and green indicate uncertainty in future $NPP_{crit,bio+ant}$ resulting from the projected anthropogenic water use and WUE, respectively. The horizontal black arrow indicates the future NPP change by 2050 from the GCMs. The red dots are satellite-observed NPP and ET. The horizontal and vertical axes have different scales before and after the breaks.

we attributed 67 ± 53% of the satellite-derived ET trend over the study area to new planting.

The reduction in runoff from revegetation affects the amount of water available for human activities, with the potential for adverse socio-economic consequences[7]. Here we define the threshold of the regional vegetation capacity by subtracting human water demand from the precipitation, as the permissible NPP for the coupled anthropogenic–biological system (see Methods for details of the calculation of this threshold of NPP, $NPP_{crit,bio+ant}$). The minimum amount of water needed for maintaining socio-economic activities across the Loess Plateau is estimated as 17 ± 2 mm yr^{-1} (see Methods and Supplementary Notes). The human water consumption in the Loess Plateau has already exceeded the amount generated from this area, in line with the observations that the river flow at Huayuankou Station (outlet of Loess Plateau) has tended to be lower than that at Lanzhou Station (inlet of Loess Plateau) in the 2000s (Supplementary Fig. 2). The value of permissible NPP in the current climate conditions is about 395–405 g C m^{-2} yr^{-1}. This is the level of vegetation restoration that would ensure water security at current levels of human withdrawal. We estimated using the method above that by 2008 the actual NPP had already reached 400 g C m^{-2} yr^{-1}. Hence, the current amount of revegetation seems to already be above the threshold where additional vegetation plantation will cause a shortfall in the water supply for human activities—an unsustainable situation.

Using model (Coupled Model Intercomparison Project Phase 5 (CMIP5)) projections for the climate over the region for the greenhouse gas concentration pathway (RCP) RCP4.5 (ref. 6) and a projected water demand increase of 46% from the national report on sustainable water resources strategy (ref. 17), we estimated permissible NPP changes by 2050 (2041–2050). The 30 climate models show regional precipitation changes in the range −9% to +14% by 2050, indicating a large uncertainty (23 of the models show increased precipitation and 7 of the models show decreased precipitation compared with the decade of the 2000s, the period that annual precipitation insignificantly increased with a trend of 4.5 mm yr^{-2} ($p = 0.37$)). This translates into future climate change modifying permissible NPP from an increase of 128 g C m^{-2} yr^{-1} to a decrease of −117 g C m^{-2} yr^{-1} (Fig. 3). This range of permissible NPP reflects the different precipitation projections from the CMIP5 models. The results under other RCPs (see Supplementary Figs 5–7) are similar to those under the RCP4.5 pathway.

It should be noted that the precipitation-induced changes of permissible NPP may be partly ameliorated by the increased plant water-use efficiency (WUE) under rising atmospheric CO_2 concentration and climate change[18–20]. We estimated future changes in WUE using the NPP-to-ET ratio of those CMIP5 land surface models, which take into account climate change and CO_2 fertilization. These land surface models project an average increase of WUE of 10% by 2050[6], which translates into an extra permissible NPP increase of 42 g C m^{-2} yr^{-1} (see green dashed line in Fig. 3). In the maximum, median and minimum scenarios of precipitation change, permissible NPP by 2050 is then 578 ± 48 g C m^{-2} yr^{-1}, 473 ± 41 g C m^{-2} yr^{-1} and 309 ± 29 g C m^{-2} yr^{-1}, respectively. This is also comparable to the NPPs predicted by the CMIP5 global climate models (GCMs) (383–464 g C m^{-2} yr^{-1}) under the RCP4.5 climate scenario shown in Fig. 3 (see Methods).

The Chinese government plans to invest another US$9.5 billion in GTGP on the Loess Plateau by 2050 (see Supplementary Notes)[5].

Our analyses suggest that although this programme has contributed to increasing vegetation productivity, this has been at the cost of an already detectable reduction in river runoff[21,22]. Given that current vegetation productivity in this region is already close to $NPP_{crit,bio+ant}$, continuing revegetation will inevitably reduce the water available for human use to less than the amount required. At the same time, climate change and elevated CO_2 adds an uncertainty, with only a 70% chance of keeping $NPP_{crit,bio+ant}$ within 20% of its current value. IPCC AR5 has proposed revegetation and biofuel farming as efficient approaches to mitigate global warming[6]. Our result suggests that climate stabilization scenarios that include substantial bioenergy resources[23] may be overestimating the potential of vegetation plantation. As for the Loess Plateau, shrub-liked planted trees are present in many parts of this region[24], calling for a better match of vegetation species and planting density to the natural environment. Unless the water constraints are considered, integrated assessment models will probably underestimate the full economic cost of bioenergy. For the long-term success of revegetation, an evidence-based strategy is needed that recognizes both ecological and socio-economic resource demands on this coupled anthropogenic–biological system; such a policy maximizes the likelihood that the dual goals of ecological and socio-economic sustainability are met.

Methods

Methods and any associated references are available in the online version of the paper.

Received 30 September 2014; accepted 1 July 2016; published online 8 August 2016

References

1. Lal, R. Potential of desertification control to sequester carbon and mitigate the greenhouse effect. *Climatic Change* **51,** 35–72 (2001).
2. Lal, R. Carbon sequestration in dryland ecosystems. *Environ. Manage.* **33,** 528–544 (2003).
3. Menz, M. H. M., Dixon, K. W. & Hobbs, R. J. Hurdles and opportunities for landscape-scale restoration. *Science* **339,** 526–527 (2013).
4. Jackson, R. B. *et al*. Trading water for carbon with biological carbon sequestration. *Science* **310,** 1944–1947 (2005).
5. Liu, J. G., Li, S. X., Ouyang, Z. Y., Tam, C. & Chen, X. D. Ecological and socioeconomic effects of China's policies for ecosystem services. *Proc. Natl Acad. Sci. USA* **105,** 9477–9482 (2008).
6. Ciais, P. *et al*. in *Climate Change 2013: The Physical Science Basis* (eds Stocker, T. F. *et al*.) Ch. 6 (IPCC, Cambridge Univ. Press, 2013).
7. Quiggin, J. Environmental economics and the Murray–Darling River system. *Aust. J. Agric. Resour. Econ.* **45,** 67–94 (2001).
8. Wang, S. *et al*. Reduced sediment transport in the Yellow River due to anthropogenic changes. *Nature Geosci.* **9,** 38–41 (2016).
9. Chen, Y. *et al*. Balancing green and grain trade. *Nature Geosci.* **8,** 739–741 (2015).
10. Farley, K. A., Jobbágy, E. G. & Jackson, R. B. Effects of afforestation on water yield: a global synthesis with implications for policy. *Glob. Change Biol.* **11,** 1565–1576 (2005).
11. Zhao, M. F., Xiang, W. H., Peng, C. H. & Tian, D. L. Simulating age-related changes in carbon storage and allocation in a Chinese fir plantation growing in southern China using the 3-PG model. *Forest Ecol. Manag.* **257,** 1520–1531 (2009).
12. Croft, H., Chen, J. M. & Noland, T. L. Stand age effects on Boreal forest physiology using a long time-series of satellite data. *Forest Ecol. Manag.* **328,** 202–208 (2014).
13. Gates, J., Scanlon, B., Mu, X. & Zhang, L. Impacts of soil conservation on groundwater recharge in the semi-arid Loess Plateau, China. *Hydrogeol. J.* **19,** 865–875 (2011).
14. Xu, X. Z., Zhang, H. W. & Zhang, O. Development of check-dam systems in gullies on the Loess plateau, China. *Environ. Sci. Policy* **7,** 79–86 (2004).
15. Zhang, X., Zhang, L., Zhao, J., Rustomji, P. & Hairsine, P. Responses of streamflow to changes in climate and land use/cover in the Loess Plateau, China. *Wat. Resour. Res.* **44,** W00A07 (2008).
16. Liang, W. *et al*. Quantifying the impacts of climate change and ecological restoration on streamflow changes based on a Budyko hydrological model in China's Loess Plateau. *Wat. Resour. Res.* **51,** 6500–6519 (2015).
17. Qian, Z. Y. & Zhang, G. D. *Comprehensive Report on China's Sustainable Water Resources Strategy* [in Chinese] (China's Water Conservancy and Hydropower Press, 2001).
18. Drake, B. G., Gonzàlez-Meler, M. A. & Long, S. P. More efficient plants: a consequence of rising atmospheric CO_2? *Annu. Rev. Plant Biol.* **48,** 609–639 (1997).
19. Wullschleger, S. D., Tschaplinski, T. J. & Norby, R. J. Plant water relations at elevated CO_2—implications for water-limited environments. *Plant Cell Environ.* **25,** 319–331 (2002).
20. Donohue, R. J., Roderich, M. L., McVicar, T. R. & Farquhar, G. D. Impact of CO_2 fertilization on maximum foliage cover across the globe's warm, arid environment. *Geophys. Res. Lett.* **40,** 3031–3035 (2013).
21. McVicar, T. R. *et al*. Development a decision support tool for China's re-vegetation program: simulating regional impacts of afforestation on average annual streamflow in the Loess Plateau. *Forest Ecol. Manag.* **251,** 65–81 (2007).
22. Mu, X. M., Zhang, L., McVicar, T. R., Chille, B. S. & Gao, P. Estimating the impact of conservation measures on stream-flow regime in catchments of the Loess Plateau. *Hydrol. Process.* **21,** 2124–2134 (2007).
23. Rose, S. K. *et al*. Land-based mitigation in climate stabilization. *Energy Econ.* **34,** 365–380 (2012).
24. McVicar, T. R. *et al*. Parsimoniously modeling perennial vegetation suitability and identifying priority areas to support China's re-vegetation program in the Loess Plateau: matching model complexity to data availability. *Forest Ecol. Manag.* **259,** 1277–1290 (2010).

Acknowledgements

We thank F. Zhou for providing river runoff data from the hydrological catchments. This study was supported by the National Natural Science Foundation of China (nos 41390464 and 41230745), Chinese Academy of Sciences (GJHZ 1502) and the Major Programme of High Resolution Earth Observation System (30-Y30B13-9003-14/16-02). The GLDAS LSM data used were acquired as part of the mission of NASA's Earth Science Division and archived and distributed by the Goddard Earth Sciences (GES) Data and Information Services Center (DISC).

Author contributions

B.F., X.F. and S.P. designed the research. X.F., S.P., B.F., S.W. and P.C. wrote the manuscript. S.P., Z.Z., X.F. and Y. Li conducted modelling, projection and statistical analysis. Y.Z., X.F. and B.W. conducted the remotely sensed NPP, ET and land-cover analysis. Y. Lü, S.W. and X.J. conducted the analysis of river runoff from the hydrological catchments.

Additional information

Supplementary information is available in the online version of the paper. Reprints and permissions information is available online at www.nature.com/reprints. Correspondence and requests for materials should be addressed to B.F.

Competing financial interests

The authors declare no competing financial interests.

Methods

Study area. The Loess Plateau region in central China covers approximately 640,000 km^2. During the period 2000–2010, annual precipitation varied from 200 mm yr^{-1} in the northwest to 800 mm yr^{-1} in the southeast of the plateau, with a mean value 440 ± 50 mm yr^{-1}. It is a typical water-limited landscape with evaporation accounting for 85% of the precipitation; this percentage increases along the precipitation gradient. The Loess Plateau can be divided into three regions according to the water available to the ecosystem, namely: the Mu Us Desert in the driest northwest sector of the Loess Plateau; an area of irrigated agriculture within the main stem of the Yellow River catchment in the southeast Loess Plateau; and the rain-fed hilly area in the middle of the Loess Plateau. The last of these covers more than 60% of the region, with annual precipitation between 400 and 550 mm yr^{-1} (Fig. 1a). Revegetation occurred on the hilly parts of the plateau where precipitation is the only water input to the local ecosystems. Ecosystems in the Loess Plateau are water-limited, with evaporation limited by the water availability rather than by the energy input[25,26]. The dryness index, the ratio of potential evapotranspiration[27] (ET) to precipitation, is 3.0 ± 0.5 for the entire Loess Plateau and has been stable over the past few decades (see Supplementary Fig. 9 and the Supplementary Notes).

Meteorological and hydrological data. Daily meteorological data (daily average air temperature and precipitation from the National Meteorological Administration of China, http://data.cma.cn) for the period 1980–2010 were obtained from 172 stations within and near the Loess Plateau, and interpolated onto a 1-km grid covering the entire Loess Plateau using a digital elevation model and a thin-plate smoothing spline method (ANUSPLIN 3.1)[28]. Gridded annual precipitation was derived from the daily precipitation maps. Daily runoff data from 32 rivers were acquired from hydrometric observations, and converted to area-average depth-equivalents for each catchment (R, mm). Precipitation falling on each catchment was calculated from spatial fields of annual precipitation with the spatial statistical tools in ARCGIS 9.0. Multi-year averages of annual runoff and annual precipitation for each catchment in the periods 1980–2000 and 2000–2010 were used to derive the field-observed runoff–precipitation relationships before and after the GTGP revegetation. LAI derived from the Global Land Surface Satellite normalized difference vegetation index (NDVI) series of harmonized Advanced Very High Resolution Radiometer and MODIS NDVI[29] (www.landcover.org) was used to indicate variation in plant growth conditions and plant structure in the period 1982–2010.

Satellite-estimated NPP and ET. Using the terrestrial Carnegie–Ames–Stanford approach (CASA) ecosystem model, we estimated net primary production (NPP) at 1-km spatial resolution across the Loess Plateau for the period 2000–2010. The CASA NPP was calculated as the product of the modulated 'absorbed photosynthetically active radiation' (APAR) and the light-use efficiency (LUE) factor: $\mathrm{NPP}(x,t) = \mathrm{APAR}(x,t)\varepsilon(x,t)$. Here $\mathrm{NPP}(x,t)$ represents plant growth at spatial location x and time t (g C m^{-2}), and $\mathrm{APAR}(x,t)$ and $\varepsilon(x,t)$ are the canopy-absorbed incident solar radiation (MJ m^{-2}), and the LUE (g C MJ^{-1}) of APAR respectively, also at location x and time t. CASA uses satellite-observed NDVI as the driving factors, and drivers other than climate, such as CO_2 fertilization and land-use change affect satellite-observed NDVI. Thus, CASA partly indirectly considers the effect of these drivers on vegetation productivity. Some processes such as the indirect effect of CO_2 fertilization on LUE are unconsidered in CASA due to the limited knowledge. Compared with other process-based models, the CASA model has been shown to be the most effective at simulating carbon assimilation by plant growth in the Loess Plateau. CASA simulations have been shown to be comparable to observed values in the Loess Plateau[30]. NPP was calculated for each month and then summed to give the annual NPP needed in this analysis.

Satellite-estimated actual ET over the Loess Plateau for the period 2000–2010 was derived from a previous study[31]. It was estimated from the surface energy balance: $\lambda E + H = R_n - G_0$, where H (W m^{-2}) is the sensible heat flux, λE (W m^{-2}) is the latent heat flux, R_n (W m^{-2}) is the net radiation absorbed at the land surface, and G_0 (W m^{-2}) is the soil heat flux. The aerodynamic roughness integrates three contributions originating from vegetation cover, topographical terrain variation and non-vegetation obstacles respectively. λE was converted into actual ET (mm d^{-1}), using the temperature-dependent latent heat of vaporization and the density of water. To generate continuous ET data during cloudy days and for days between satellite overpasses, intermittent remote sensing data were interpolated and λE was estimated using the Penman–Monteith equation. For detailed information, see ref. 31. Daily ETs were then summed to give annual ET for this analysis.

Data inputs required for the satellite-estimated NPP and ET include land cover, 8-day composite of 1-km MODIS NDVI, and spatial temperature and precipitation fields. Land cover data for the Loess Plateau before and after the GTGP (derived from maps in years 2000 and 2008, respectively) were extracted from Landsat Enhanced Thematic Mapper. MODIS NDVI data were acquired from the MODIS Land Processes Distributed Archive Center.

Water balance ET and GLDAS soil moisture. To confirm whether or not the trend of ET in the Loess Plateau is significant, we applied a water balance equation to estimate annual ET from the Loess Plateau between 2000 and 2010. The yearly water balance equation is:

$$\mathrm{ET} = PPT - (R_{\mathrm{out}} - R_{\mathrm{in}}) - \Delta\mathrm{RW} - \Delta\mathrm{SW} - \Delta\mathrm{GW} \quad (1)$$

where PPT, R_{out}, R_{in}, ΔRW, ΔSW and ΔGW are annual: precipitation, outflow, inflow, changes in river-reservoir water storage, in soil water storage and in groundwater withdrawal for plant growth, respectively. PPT, R_{out} and R_{in} data were obtained from meteorological and hydrological stations. ΔRW in the Loess Plateau is from data reported by the Chinese Ministry of Water Resources (Yellow River Water Resources Bulletin, http://www.yellowriver.gov.cn/other/hhgb). ΔSW is from the Global Land Data Assimilation System (GLDAS; http://disc.sci.gsfc.nasa.gov/hydrology/data-holdings). Vegetation in the Loess Plateau is mostly rain-fed. Especially in the loess area where revegetation occurred, both groundwater recharge and groundwater discharge are difficult to estimate since soil depth in these areas is 100 ∼ 200 m on average with the maximum exceeding 300 m (ref. 32). About 0.8% of the Loess Plateau area is irrigated with groundwater. The underground water-irrigated area is about 0.8% of the Loess Plateau area (see Supplementary Notes). Because of this small area of groundwater irrigation, ΔGW was set to zero in the calculation.

Regional *in situ* soil moisture data do not exist for the Loess Plateau over the long period of 1980–2010; we therefore used the time series of soil moisture estimated by the Community Land Model GLDAS. These estimates are for the depth between the surface and 3.2 m. Vegetation specifications used in GLDAS include satellite-derived products of LAI and canopy greenness; thus, surface greening due to plantations has already been accounted for in the GLDAS product. We further confirmed the applicability of the variation in GLDAS soil moisture by applying it in equation (1) to estimate annual ET from the Loess Plateau. These calculations lead to a value comparable to the satellite-derived ET in our study. Using the GLDAS product, we found that annual ΔSW is not zero, although ΔSW equals zero would be expected in an ecosystem in hydrological equilibrium. We found a systematic, significant and negative trend in the soil moisture over Loess Plateau ($p < 0.001$) implying that the ecosystem was mining soil water, which is consistent with the reported soil desiccation in the Loess Plateau that has been attributed to the excessive depletion of deep soil water by planted vegetation and long-term insufficient precipitation input[33]. Therefore, soil moisture change cannot be ignored in translating the observed reduction of annual runoff into an increase of ET. However, neither the GRACE-derived groundwater storage anomaly nor the annual variation of the water table of the Loess Plateau changed significantly during the period ($p > 0.1$, see Supplementary Fig. 10 and Supplementary Notes).

GEM-estimated NPP and ET. Different process-based ecosystem models: LPJ (the Lund–Potsdam–Jena model)[34]; LPJ_GUESS (the Lund–Potsdam–Jena General Ecosystem Simulator)[35]; ORCHIDEE (the Organising Carbon and Hydrology in Dynamic Ecosystems model)[36] and CLM4CN (the Community Land Model version 4 extended with carbon–nitrogen biogeochemical model)[37] were used to quantify the contribution from climate change and rising atmospheric CO_2 concentration to the change in annual NPP and ET over the study area. All models (except CASA) performed simulations using historical climate fields from the CRU-NCEP (Climatic Research Unit, National Centers for Environmental Prediction) v4 data set (http://www.esrl.noaa.gov/psd/data/gridded/data.ncep.reanalysis.pressure.html) and global atmospheric CO_2 concentration (http://cdiac.ornl.gov/ftp/trends/co2/maunaloa.co2). These models have been widely used to investigate regional and global terrestrial carbon cycles, and have been partly validated against observations across different ecosystems and regions, including China[38–41]. In response to rising atmospheric CO_2 concentration, modelled NPP increases are comparable to those measured using free-air carbon enrichment experiments[42]. These models have also been applied to detect and attribute change in vegetation growth[43–45] and runoff[46,47] at the regional and continental scale, including China[48].

Anthropogenic water demand. Water consumption by socio-economic systems was acquired from the statistics published by the Ministry of Water Resources. Water demand data for domestic use, industry, fishing and animal husbandry were included in the analysis, but agricultural irrigation was excluded because it was included in the ET loss from the cropland NPP. Since current groundwater withdrawal, which makes up 30% of human water demand, is unsustainable in the Loess Plateau (see Supplementary Notes), we assume that human water demand is all taken from runoff.

Critical NPPs and the projection into the future. We calculated a linear regression relating annual ET to annual NPP of the Loess Plateau. The important permissible NPP threshold ($\mathrm{NPP}_{\mathrm{crit,bio+ant}}$) is reached when the water needed for

vegetation productivity and the water consumption by socio-economic systems can only just be met from the annual precipitation. In addition, we also estimated $NPP_{crit,bio+ant}$ under future (by 2050) climate using the output of 30 global climate models (GCMs) from the Intergovernmental Panel on Climate Change Fifth Assessment Report under the different greenhouse gas concentration pathways of RCP4.5, RCP2.6, RCP6.0 and RCP8.0[49,50]. In each scenario, the $NPP_{crit,bio+ant}$ under maximum, median and minimum scenarios (Fig. 3 blue lines) are estimated by the maximum, median and minimum relative precipitation change of the 30 GCMs. Future permissible NPP is also regulated by the changes in water-use efficiency (WUE), that is, NPPs′ = NPPs(WUE(2040s)/WUE(2010s)), where WUE is calculated from the average NPP-to-ET ratio from the seven GCMs that include both NPP and ET. We also compared permissible NPP in the 2050s with NPP in the 2050s predicted by the CMIP5 GCMs. Note that considering the large difference in magnitude of NPP between CMIP5 GCMs and CASA, we estimated NPP in the 2050s by multiplying the current CASA-estimated NPP by the relative NPP change rate derived from GCMs. Under the scenario of RCP4.5, GCMs generally predict increasing NPP at a rate ranging from 2.6 to 24.4%.

Statistical analysis. We calculated linear regressions relating series of each of annual NPP and annual ET with time (year y). Regression coefficient b was calculated as:

$$b = \frac{\sum_{i=1}^{9}(w_i - \bar{w})(y_i - \bar{y})}{\sum_{i=1}^{9}(w_i - \bar{w})^2} \quad (2)$$

where i is the sequential year. For each of the dependent variables, w_i is the annual NPP, annual ET or MODIS NDVI for year i, and $\bar{w}$ and $\bar{y}$ are the mean values. The regression coefficient b was then used to predict the trends of annual NPP, annual ET or MODIS NDVI since the implementation of the GTGP.

References

25. Rodà, F., Retana, J., Gracia, C. A. & Bellot, J. *Ecology of Mediterranean Evergreen Oak Forests* (Springer, 1999).
26. Budyko, M. I. *Climate and Life* (Academic, 1974).
27. Liu, Q. & McVicar, T. R. Assessing climate change induced modification of Penman potential evaporation and runoff sensitivity in a large water-limited basin. *J. Hydrol.* **464,** 352–362 (2012).
28. McVicar, T. R. *et al*. Spatially distributing monthly reference evapotranspiration and pan evaporation considering topographic influences. *J. Hydrol.* **338,** 196–220 (2007).
29. Zhao, X. *et al*. The Global Land Surface Satellite (GLASS) remote sensing data processing system and products. *Remote Sens.* **5,** 2436–2450 (2013).
30. Feng, X. M., Fu, B. J., Lu, N., Zeng, Y. & Wu, B. F. How ecological restoration alters ecosystem services: an analysis of carbon sequestration in China's Loess Plateau. *Sci. Rep.* **3,** 2846 (2013).
31. Wu, B. F. *et al*. Validation of ETWatch using field measurements at diverse landscapes: a case study in Hai Basin of China. *J. Hydrol.* **436–437,** 67–80 (2012).
32. Chen, X. D. *Hydrology of Yellow River Basin* [in Chinese] (Yellow River Water Conservancy Press, 1996).
33. Chen, H. S., Shao, M. A. & Li, Y. Y. Soil desiccation in the Loess Plateau of China. *Geoderma* **143,** 91–100 (2008).
34. Sitch, S. *et al*. Evaluation of ecosystem dynamics, plant geography and terrestrial carbon cycling in the LPJ dynamic global vegetation model. *Glob. Change Biol.* **9,** 161–185 (2003).
35. Hickler, T. *et al*. Using a generalized vegetation model to simulate vegetation dynamics in northeastern USA. *Ecology* **85,** 519–530 (2004).
36. Krinner, G. *et al*. A dynamic global vegetation model for studies of the coupled atmosphere-biosphere system. *Glob. Biogeochem. Cycles* **19,** GB1015 (2005).
37. Lawrence, D. M. *et al*. Parameterization improvements and functional and structural advances in version 4 of the community land model. *J. Adv. Model. Earth Syst.* **3,** M03001 (2011).
38. Tan, K. *et al*. Application of the ORCHIDEE global vegetation model to evaluate biomass and soil carbon stocks of Qinghai-Tibetan grasslands. *Glob. Biogeochem. Cycles* **24,** GB1013 (2010).
39. Tao, F. & Zhang, Z. Dynamic responses of terrestrial ecosystems structure and function to climate change in China. *J. Hydrometeorol.* **12,** 371–393 (2011).
40. Peng, S. *Global Change Impacts on Forest Ecosystems in East Asia* (Peking University, 2012).
41. Peng, S. *et al*. Precipitation amount, seasonality and frequency regulate carbon cycling of a semi-arid grassland ecosystem in Inner Mongolia, China: a modeling analysis. *Agric. For. Meteorol.* **178,** 46–55 (2013).
42. Piao, S. *et al*. Evaluation of terrestrial carbon cycle models for their response to climate variability and to CO_2 trends. *Glob. Change Biol.* **19,** 2117–2132 (2013).
43. Lucht, W. *et al*. Climatic control of the high-latitude vegetation greening trend and Pinatubo effect. *Science* **296,** 1687–1689 (2002).
44. Piao, S. *et al*. Effect of climate and CO_2 changes on the greening of the Northern Hemisphere over the past two decades. *Geophys. Res. Lett.* **33,** L23402 (2006).
45. Mao, J. *et al*. Global latitudinal-asymmetric vegetation growth trends and their driving mechanisms: 1982–2009. *Remote Sens.* **5,** 1484–1497 (2013).
46. Piao, S. L. *et al*. Climate and land use changes have a larger direct impact than rising CO_2 on global river runoff trends. *Proc. Natl Acad. Sci. USA* **104,** 15242–15247 (2007).
47. Shi, X., Mao, J., Thornton, P. E., Hoffman, F. M. & Post, W. M. The impact of climate, CO_2, nitrogen deposition and land use change on simulated contemporary global river flow. *Geophys. Res. Lett.* **38,** L08704 (2011).
48. Piao, S. L. *et al*. Detection and attribution of vegetation greening trend in China over the last 30 years. *Glob. Change Biol.* **21,** 1601–1609 (2015).
49. Meinshausen, M. *et al*. The RCP greenhouse gas concentrations and their extensions from 1765 to 2300. *Climatic Change* **109,** 213–241 (2011).
50. Taylor, K. E., Stouffer, R. J. & Meehl, G. A. An overview of CMIP5 and the experiment design. *Bull. Am. Meteorol. Soc.* **93,** 485–498 (2012).